International Journal of Mass Spectrometry 308 (2011) 181–190

Contents lists available at ScienceDirect

International Journal of Mass Spectrometry

journal homepage: www.elsevier.com/locate/ijms

Formation of molecular hydrogen from protonated 9,10-dihydroanthracene: Is the ejected H_2 rotationally and vibrationally excited?

Martin Vala [a,*], Jan Szczepanski [a], Jos Oomens [b,c]

[a] Department of Chemistry and Center for Chemical Physics, P.O. Box 117200, University of Florida, Gainesville, FL 32611-7200, United States
[b] FOM Institute for Plasma Physics "Rijnhuizen", Edisonbaan 14, NL-3439MN Nieuwegein, The Netherlands
[c] van't Hoff Institute for Molecular Sciences, University of Amsterdam, Science Park 904, NL-1098XH Amsterdam, The Netherlands

ARTICLE INFO

Article history:
Received 4 April 2011
Received in revised form 12 May 2011
Accepted 13 June 2011
Available online 21 June 2011

Keywords:
Infrared multiple-photon dissociation
Astrochemistry
Molecular hydrogen formation
Density functional calculations
Protonation of dihydroanthracene

ABSTRACT

The infrared multiple-photon dissociation (IRMPD) spectrum of protonated 9,10-dihydroanthracene ($[DHA+H]^+$, m/z 181) has been recorded using an infrared free electron laser. Protonation was accomplished by electrospray ionization with subsequent mass-selection and trapping in a Fourier transform ion cyclotron mass spectrometer. IR-induced fragment ions were observed at m/z 179, 166, and 165. Density functional calculations (B3LYP/6-311++G(d,p)) of the infrared spectra of the two possible protonated isomers of DHA showed that the observed IRMPD spectrum is best fit to a mixture of the two isomers. Potential energy surfaces for the loss of atomic and molecular hydrogen from the aliphatic carbons of $[DHA+H]^+$ have been calculated. The lowest energy barriers are for loss of H_2. After H_2 ejection, stabilization of the remaining fragment occurs by hydrogen migration from one of the aliphatic carbons to the bare ejection site. In all cases the stabilized fragment is computed to be 9-hydroanthracene. The IRMPD spectrum of the m/z 179 fragment has been recorded and is shown to correspond closely both to the calculated and previously recorded IRMPD spectrum of ionic 9-hydroanthracene. The highly asymmetric transition state conformation of the to-be-formed H_2 and the remaining fragment is highly suggestive of rotational, vibrational, and, possibly, translational excitation of the ejected H_2. Evidence for such excitation from astronomical observations that show the close proximity of PAHs and H_2 in certain interstellar objects and that show H_2 rotational excitation, which has been difficult to explain via either collisional activation or UV pumping, is reviewed.

1. Introduction

Molecular hydrogen is an unusual species even though it is composed of the most abundant element in the universe and is the simplest neutral molecule known. Despite many observational and theoretical studies of its properties, the mechanism of formation of H_2 in the interstellar medium (ISM) remains a subject of intense debate.

The formation of H_2 in the ISM has been widely thought to occur on the surface of dust grains, as proposed over 45 years ago by Gould and Salpeter [1]. One of two mechanisms of H_2 formation on grains is usually invoked: the Eley–Rideal mechanism, in which an incoming H atom directly abstracts another H atom trapped on the grain surface, or the Langmuir–Hinshelwood mechanism, in which H atoms captured on the grain surface migrate until encountering each other and combining. Much effort has gone into the development of these processes. Recently, a number of groups have suggested that polycyclic aromatic hydrocarbons (PAHs), rather than dust grains, could act as catalysts for the formation of H_2. This idea, floated by Omont [2], Bohme [3], Cassam-Chenai et al. [4], and Pauzat and Ellinger [5], was later investigated theoretically by a number of groups. Essentially invoking the Eley–Rideal mechanism, Bauschlicher [6] and Hirama et al. [7] reported independent calculations on a number of PAHs, including naphthalene, anthracene, pyrene, and coronene, and showed that the addition of the first H atom to a PAH cation is exothermic and that the abstraction of this H by a second incoming H to yield H_2 proceeds with a zero or small activation barrier, permitting the reaction to proceed at very low temperatures. Rauls and Hornekaer [8] calculated low (or zero) energy barriers for the addition of one or multiple H atoms onto neutral coronene and showed that H_2 could readily form via the Eley–Rideal abstraction reaction, both from edge carbons and inner ring carbons. They also pointed out that superhydrogenated PAHs could exist in the ISM in regions of low UV flux. Joblin and coworkers [9] investigated another pathway for H_2 formation, in which two hydrogen atoms at nearby carbons in naphthalene react, followed by their bonding and removal. Le Page and coworkers [10] proposed an alternative mechanism, the dissociative

* Corresponding author. Tel.: +1 352 392 0529; fax: +1 352 392 0872.
E-mail address: mvala@chem.ufl.edu (M. Vala).

1387-3806/$ – see front matter © 2011 Elsevier B.V. All rights reserved.
doi:10.1016/j.ijms.2011.06.008

recombination of a hydrogenated PAH cation with an electron, and in calculating the rate of H_2 formation found that the predicted rate of formation was in good accord with the rate generally inferred from standard astrochemical models.

In this paper, we report on an infrared multiple-photon dissociation spectral and theoretical study of protonated 9,10-dihydroanthracene ($[DHA+H]^+$). DHA is fundamentally different from the other H_2-forming PAHs we have studied, *viz.*, 1,2-dihydronaphthalene [11], acenaphthene, and 9,10-dihydrophenanthrene [12], all of which contain *adjacent* aliphatic carbon atoms (before protonation), which DHA does not. It is of interest to determine whether adjacent aliphatic carbons are necessary for H_2 formation on PAH centers. From our studies of PAHs with multiple aliphatic carbons, we propose a model for the formation of molecular H_2 which is different from the above mentioned models. We show that the excitation of a hydrogenated PAH enables the formation of H_2 by the extraction of two hydrogens, either from the same aliphatic carbon or from nearby ones, that the presence of more than one aliphatic center enables hydrogen migration around the PAH rings, thereby stabilizing the remaining fragment, and that the H_2 very likely is ejected rotationally, vibrationally, and translationally excited. It is pointed out that the excitation of H_2 may be pertinent to a number of astronomical observations.

2. Methods

2.1. IRMPD experiment

Recent developments in the field of ion spectroscopy have greatly expanded the experimental information obtainable on gas phase ion structure and reactivity. In particular, the coupling of tandem mass spectrometers (such as Fourier-transform ion cyclotron resonance mass spectrometers (FTICR-MS)) with free electron lasers with tunable output in the infrared (such as the Free Electron Laser for Infrared eXperiments (FELIX) [13]) has enabled detailed information to be gotten on the infrared vibrational frequencies of many gaseous ions [14,15]. The experimental apparatus has been previously described [16,17]. Protonated 9,10-dihydroanthracene ($[DHA+H]^+$) was formed by electrospray ionization of an 80:20:0.02 methanol/water/ammonium acetate solution of ~5 mM neutral DHA with an infusion rate of ~10 μL/min. Trapped ions were exposed to 5 μs long laser macropulses (50 mJ, 10 Hz repetition rate, 6.4 s duration). Each macropulse consists of a train of approximately 1 ps long pulses separated by 1 ns. For protonated DHA (*m*/*z* 181), observed IRMPD fragment peaks appear at *m*/*z* 179, 166, and 165. To enhance the yield of fragment ions, a CO_2 laser (10.6 μm, CW, 25 W) was directed at the trapped ion cloud and triggered on at the trailing edge of each FELIX macropulse for a duration of 50 ms.

The infrared multiple photon dissociation (IRMPD) spectrum was generated by plotting the intensity of the three fragment peaks (*m*/*z* 179,166, 165) ratioed against the total ion intensity (*m*/*z* 181 parent plus fragments) as a function of FELIX photon energy. An IRMPD spectrum was also recorded for the mass-selected *m*/*z* 179 fragment by monitoring the increase of the fragment obtained by the loss of one hydrogen atom (*m*/*z* 178).

2.2. Calculations

2.2.1. Infrared spectra

The equilibrium geometries and harmonic vibrational frequencies for $[DHA+H]^+$ were calculated using density functional theory with the Gaussian 03 program package [18]. Becke's three-parameter hybrid functional, the non-local correction functional of Lee, Yang, and Parr (B3LYP), with a 6-311++G basis set and d and p polarization functions on heavy and hydrogen atoms, respectively, was applied. The IRMPD spectra have been modeled using B3LYP/6-311++G(d,p) harmonic vibrational calculations. The vibrational frequencies were scaled uniformly by a factor of 0.98 to correct for anharmonicity effects and functional/basis set deficiencies. This empirically established scaling factor was adopted from our previous work [19] where a similar level of theory was used successfully.

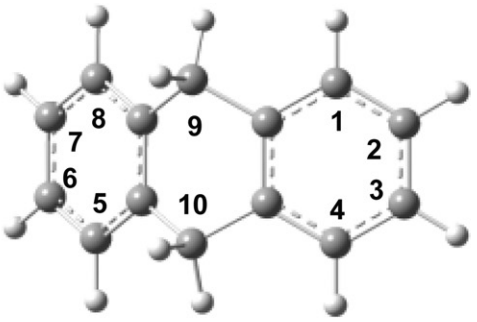

9,10-dihydroanthracene (DHA)
$C_{14}H_{12}$, $^1A_1$, C_{2v}

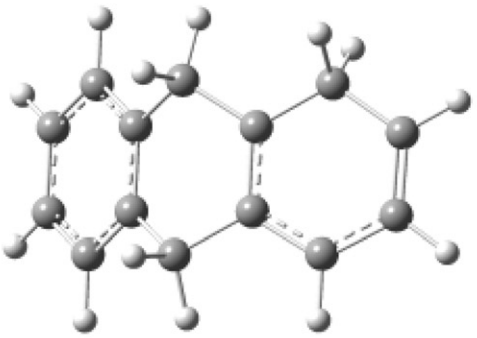

DHA protonated at site 1, $[DHA+H(1)]^+$
$C_{14}H_{13}^+$, ^1A, C_1

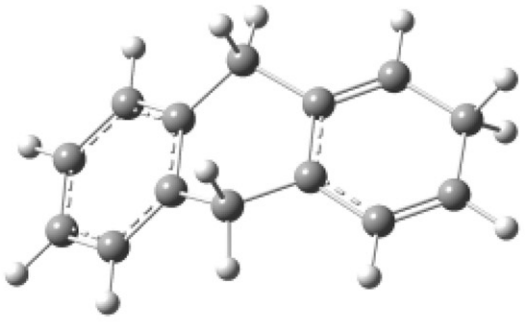

DHA protonated at site 2, $[DHA+H(2)]^+$
$C_{14}H_{13}^+$, ^1A, C_1

Fig. 1. Equilibrium geometries of 9,10-dihydroanthracene (DHA) and its protonated stable isomers $[DHA+H(1)]^+$ and $[DHA+H(2)]^+$, computed at the B3LYP/6-311++G(d,p) level.

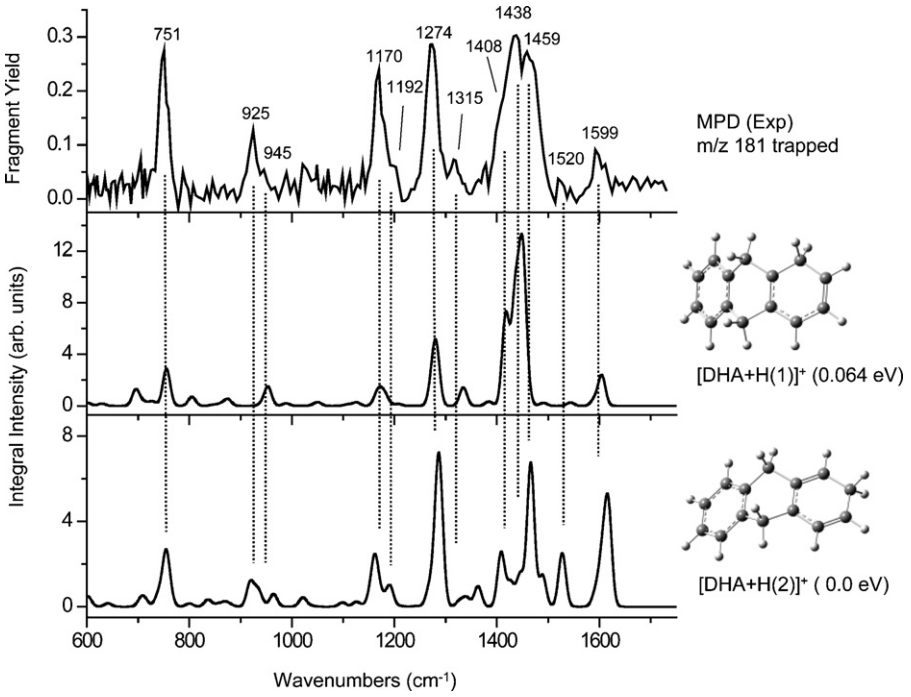

Fig. 2. Experimental IRMPD spectra of protonated DHA (*m*/*z* 181 trapped) (top panel) compared to predicted vibrational spectra (B3LYP/6-311++G(d,p) level) of two protonated DHA isomers. The relative ZPE-corrected isomer electronic energies are indicated.

2.2.2. Potential energy surfaces for H_2 formation

For the H_2 ejection reactions, transition states (TS) connecting the stable minima on the potential energy surfaces were sought by applying the QST3 optimization procedure in Gaussian 03 [15]. The B3LYP/6-31G(d,p) functional/basis set was used. The harmonic vibrational frequencies were calculated for each structure involved in the PES calculation in order to verify whether a first order TS was present. The electronic energies in the PES figures (*vide infra*) were ZPE-corrected without scaling. We note that a similar level of calculation was previously applied in PES studies of the H_2 and H dissociative loss from the naphthalene cation [9].

3. Results and discussion

3.1. Proton affinities

There are two unique sites on 9,10-dihydroanthracene (DHA) to which a proton may attach (1 and 2, see Fig. 1). The computed proton affinities for the two sites are very close in energy (8.36 eV for position 1 and 8.42 eV for position 2). The stabilities of the ground states of these two protonated isomers are also similar. Proton attachment at position 2 yields an isomer ($[DHA+H(2)]^+$) which is slightly more stable (by 0.064 eV) than $[DHA+H(1)]^+$ (see Fig. 2a).

3.2. Mass spectrometry and IRMPD spectroscopy

Fig. 2 shows the experimental IRMPD spectrum for $[DHA+H]^+$ together with the computed IR spectra for its two possible isomers. Although the predicted IR spectra for both isomers correspond roughly to the observed spectrum (see Table 1), there are some differences which favor the $[DHA+H(2)]^+$ isomer. In the 925/945 cm^{-1} region, the $[DHA+H(1)]^+$ spectrum has only one band while the $[DHA+H(2)]^+$spectrum shows two, possibly three. The same holds true in the 1170/1192 cm^{-1} region. The 1408/1438/1459 cm^{-1} region is particularly informative. Neither isomer predicts the band structure of this region particularly well. Because the ground state energies of the isomers are close, both isomers may contribute to the observed spectrum. To model this, we combined different percentages of the two isomeric spectra. The combination corresponding to 67% $[DHA+H(2)]^+$ to 33% $[DHA+H(1)]^+$ appeared to give the best fit to experiment, but is not considered conclusive. We therefore conclude that it appears that both isomers are present in the sample mixture in an undefined ratio. This tentative conclusion reflects the fact that relative intensities in an IRMPD spectrum may be skewed, especially when multiple bands occur in close proximity [20].

3.3. PES computations of H_2 formation from protonated DHA

One of the major questions addressed in this study was whether the loss of two mass units by the parent species to yield the *m*/*z* 179 fragment results from the loss of two H atoms or molecular H_2. To address this question, we have calculated a number of partial potential energy surfaces (PESs) for both processes. Fig. 3a shows a portion of the PES for the ejection of H_2 from carbon 9. The energies relative to the parent $[DHA+H(1)]^+$ and various intermediate structures are given in the figure. From the optimized starting structure **A**, $[DHA+H(1)]^+$, which is bent out-of-plane around the 9,10 axis, it requires 3.306 eV to mount the **TS1** transition state to reach **B**, a loosely bound complex, in which the H_2 has been asymmetrically extracted from carbon 9. In the complex, the hydrogen atoms in H_2 are 2.718 and 3.423 Å distant from carbon 9. The complex readily forms structure **C**, in which H_2 is now unbound. While this structure exists at an energy minimum, it has a "bare" carbon (C9) and is therefore not the most stable form possible. With an increase of 0.949 eV, one of the hydrogens on the adjacent aliphatic C1 carbon bridges to the C9 carbon in the **TS2** transition state and ultimately hops to that carbon. In an overall exothermic reaction, the 10-hydroanthracene radical cation (**D**) is produced.

The ejection of H_2 from carbon 9 in $[DHA+H(2)]^+$ is similar (see Fig. 3b). Although the energies and distances are different, this PES parallels that in Fig. 3a except for one feature, the process covering the "naked" carbon C9 in **C**. Moving through **TS2**, one of the hydrogens on aliphatic carbon 2 bridges to carbon 1 forming species **D**, the

Table 1
Experimental IRMPD spectrum of protonated 9,10-dihydroanthracene (DHA) compared to calculated IR absorption spectra of its two isomers of $[DHA+H(1)]^+$ and $[DHA+H(2)]^+$ with proposed band assignments.

IRMPD	$[DHA+H(1)]^+$		$[DHA+H(2)]^+$		Mode[c] $[DHA+H(1)]^+/[DHA+H(2)]^+$
ν_{exp}[a] (cm^{-1})	ν_{cal}[b] (cm^{-1})	Integral intensity (km mol^{-1})	ν_{cal}[b] (cm^{-1})	Integral intensity (km mol^{-1})	
751	754.9	43.9	754.6	44.7	ε + τ
	758.6[d]	7.9	764.2[d]	4.4	ε + τ + R
925			919.1	20.3	R(C2–C3)
			934.0[e]	13.6	ε + τ
945	953.4	25.0	964.4	10.3	R(C1–C2)/ε + τ
1170	1170.1	6.7	1161.9	39.3	α + β
	1177.4[f]	13.4			α + β
1192	1185.4	6.8	1191.2	17.0	α + β/α + β + R(C–C)
1274	1272.6	20.6	1268.6	15.9	α + β + R
	1278.5[g]	19.1	1283.9[g]	71.2	γ(C1) + β/γ(C2) + β
	1282.0[g]	63.4	1289.5[g]	66.6	γ(C1) + β/γ(C2) + β
1315	1335.5	19.0	1340.9	7.4	α + β
1408	1417.3	115.3	1408.3	45.0	γ(C9) + β/γ(C10) + β
1438	1436.0	148.7	1426.8	19.7	γ(C10) + β/γ(C9) + β
	1450.1[h]	208.1	1445.4[h]	26.3	γ(C10) + β/γ(C9) + β
1459	1460.9	11.0	1466.1	118.1	α + β + R
1520			1527.4	44.5	R + α + β
1599	1604.6	41.0	1605.6	37.9	R + α + β
			1617.1[i]	82.1	R + α + β

[a] Fig. 2, this work.
[b] Vibrational frequencies of calculated (at B3LYP/6-311++G(d,p)) spectrum are scaled uniformly by factors of 0.98.
[c] Notation used: ε and τ are CCC and CCH out-of-plane, α and β are CCC and CCH in-plane bending, γ are HC(sp^3)H scissors, while R and r are CC and CH stretching modes, respectively.
[d] Contributes to the 751 cm^{-1} band intensity in IRMPD spectrum of Fig. 2.
[e] Contributes to the 925 cm^{-1} band intensity in IRMPD spectrum of Fig. 2.
[f] Contributes to the 1170 cm^{-1} band intensity in IRMPD spectrum of Fig. 2.
[g] Contributes to the 1274 cm^{-1} band intensity in IRMPD spectrum of Fig. 2.
[h] Contributes to the 1438 cm^{-1} band intensity in IRMPD spectrum of Fig. 2.
[i] Contributes to the 1599 cm^{-1} band intensity in IRMPD spectrum of Fig. 2.

same radical (**C**) as in Fig. 3a, and then hops from C1 to C9. Although H_2 formation from the two hydrogens on C9 in either $[DHA+H(1)]^+$ or $[DHA+H(2)]^+$ requires mounting a barrier of 3–4 eV, both reactions are exothermic and both produce the 10-hydroanthracene radical cation. In a later section we show that the *m*/*z* 179 product observed after the loss of two mass units from protonated DHA is indeed the 10-hydroanthracene radical cation.

Before protonation, carbons 9 and 10 in DHA are equivalent, but with protonation in either position 1 or 2, they become inequivalent. We have thus also considered the ejection of H_2 from carbon 10 in $[DHA+H(1)]^+$ (Fig. 4a) and $[DHA+H(2)]^+$ (Fig. 4b). The initial steps are analogous to those shown in Fig. 3 for H_2 ejection from carbon 9. An energy barrier of 3.872 eV must be mounted in $[DHA+H(1)]^+$ to reach **TS1** (3.281 eV for $[DHA+H(2)]^+$). But after formation of a loose complex (structure **C**, in Fig. 4a and b), the process of covering the bare carbon C10 now involves multiple H atom hops. In Fig. 4a, one of the hydrogens on C1 jumps to C2 (after an input of 0.637 eV) forming **D** (equivalent to **C** in Fig. 4b). Continuing its hopping around the six-membered ring, it next jumps to C3 (with an input of 1.054 eV) forming structure **D** in Fig. 4b (equivalent to **C** in Fig. 3b). As we have seen above, the H then jumps to C4 (giving the equivalent of structure **D** in Fig. 3b or **C** in Fig. 3a). From there it completes the circuit to the bare carbon finally forming **D** (in Fig. 3a), the 10-hydroanthracene (or equivalently, 9-hydroanthracene) radical cation (Table 2).

Summarizing, once H_2 is extracted from carbon 10 in either protonated isomer of DHA, one of the hydrogens on the remaining aliphatic carbon on the outer ring undergoes a series of successive 1,2-hydrogen shifts forming the final product, the 10-hydroanthracene radical cation.

To the present we have only considered H_2 formation with hydrogens originating from the same aliphatic carbon, but we now consider formation of H_2 by bonding one H from C9 and one from C10. Fig. 5a displays the results of the PES calculations for $[DHA+H(2)]^+$. Recalling that the optimized structure for $[DHA+H(2)]^+$ is butterfly-bent around the C9–C10 axis, there are several vibrations in which the CH_2 groups at positions 9 and 10 rock toward each other. With a modest energy input (2.03 eV), a transition state (**TS1**) can be mounted where the nearest hydrogens attract each other and lengthen their respective CH bond lengths. As these hydrogens continue their bonding and finally break their respective CH bonds, H_2 is formed with an energy stabilization of 1.893 eV. Interestingly, no loose complex is formed as in the previous cases where H_2 is formed from two hydrogens from the same carbon. The resulting structure (**B**), 2-hydroanthracene cation, is not the lowest energy protonated form of anthracene. A series of hydrogen atom transfers, first from C2 to C1 and then from C1 to C9 ensues, leading to the most stable form, the 9-hydroanthracene ion, **D**.

The above description of H_2 formation involves simultaneous, asymmetric attractive motion of hydrogens H9 and H10. Another pathway involving stepwise motion of only one of these hydrogens

Table 2
Total energy barriers, E_b, for formation of molecular hydrogen (H_2) and 9-hydroanthracene cation (HA^+) from the protonated 9,10-dihydroanthracene (DHA) isomers, $[DHA+H(1)]^+$ and $[DHA+H(2)]^+$.

Sites	Supplied H's E_b (eV) H_2 formation	E_b (eV) HA^+ formation	PES figure number
$[DHA+H(1)]^+$			
9	**3.306**	**4.255**	3a
10	3.872	6.119	4a, 4b cont., 3b cont.
$[DHA+H(2)]^+$			
9	3.944	5.449	3b, 3a cont.
10	**3.281**	4.891	4b, 3b cont., 3a cont.
9 and 10	**2.030**	**3.898**	5a
9 and 10	**3.134**[a]	4.997[a]	5b, 5a[b]

Low energy barriers are indicated in bold.
[a] Not ZPE corrected.
[b] ZPE corrected for Fig. 5a only.

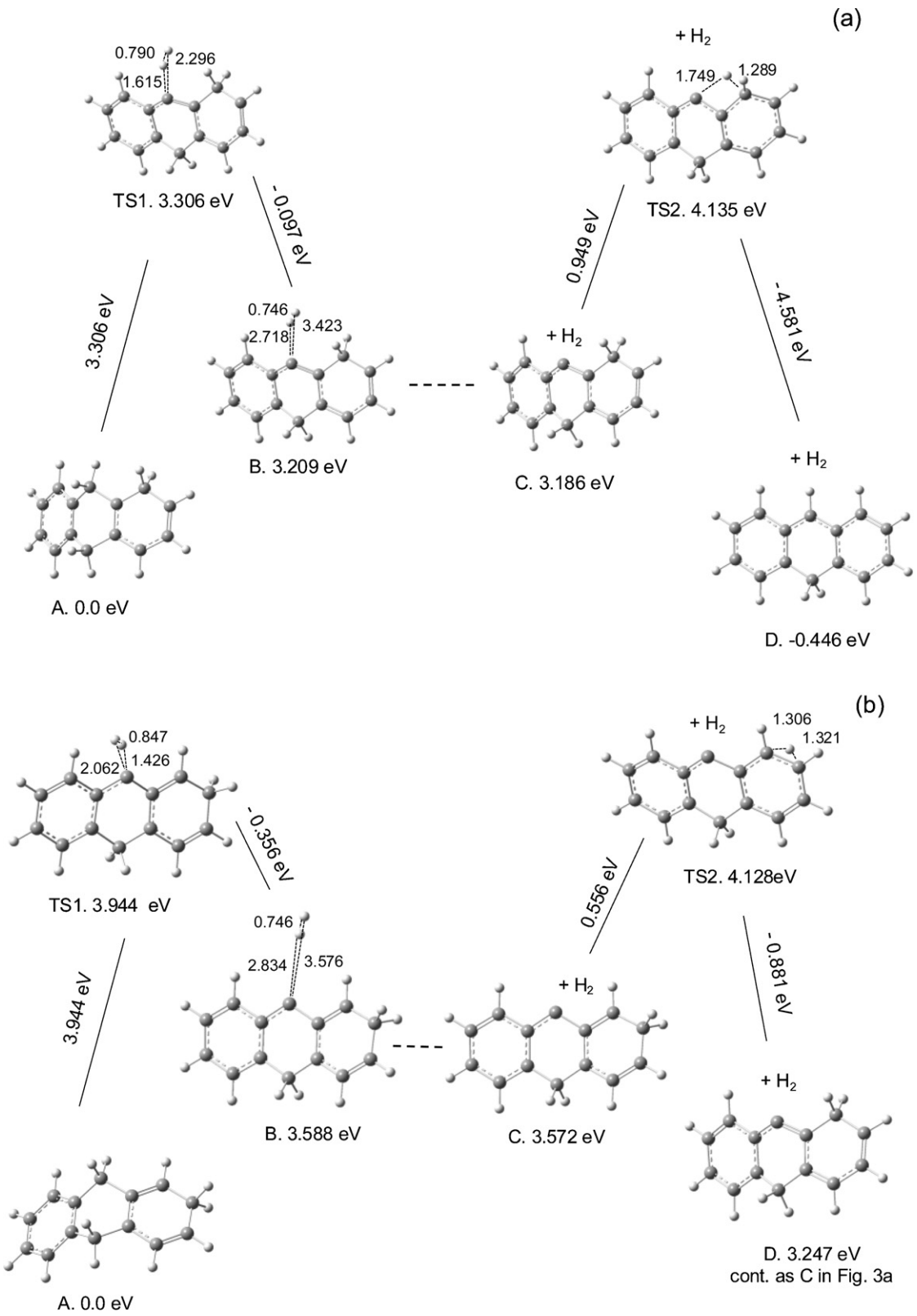

Fig. 3. Relative energy level diagram for the dissociation of molecular hydrogen from protonated DHA calculated at the B3LYP/6-31G(d,p) level. (a) Both Hs are removed from C9 of $[DHA+H(1)]^+$. (b) Both Hs are removed from C9 of $[DHA+H(2)]^+$. In both (a) and (b), cationic 9-hydroanthracene is predicted as the final product.

was investigated. This calculation is shown in Fig. 5b. As the C9H9 bond length is increased from 1.101 to 2.101 Å, the energy barrier climbed is 3.134 eV. At each step in this computation the structure was optimized except for the C9H9 bond length. But, in the next step (C9H9 bond length fixed at 2.201 Å), the energy drops precipitously to 1.500 eV. It was not possible to optimize this structure. However, by unlocking the C9H9 bond length and allowing full optimization, the structure shown at 0.455 eV (0.139 eV ZPE-corrected) was obtained. No complex with H_2 was found between the structures at 3.134 eV and 0.455 eV on this PES. The distances found for

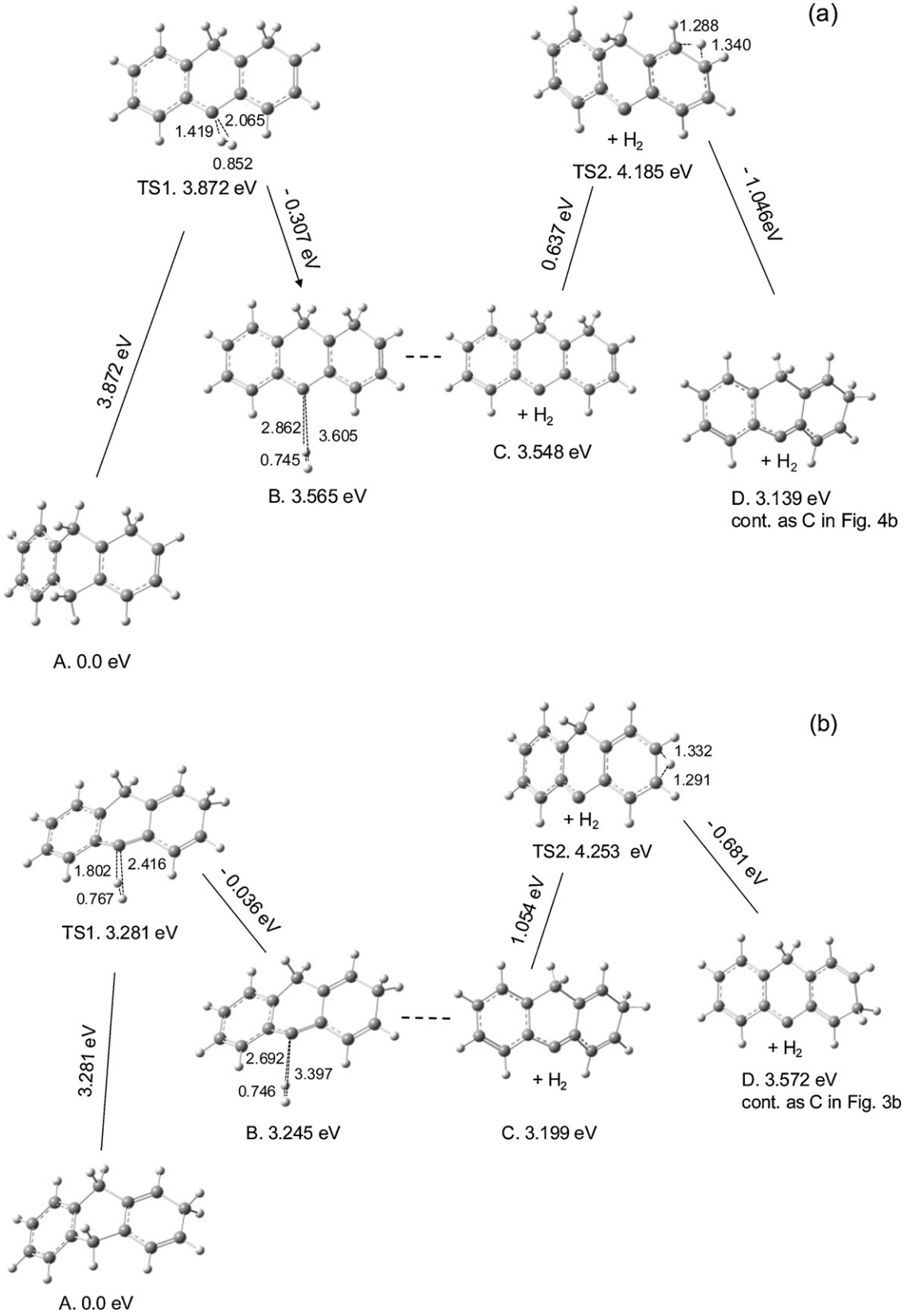

Fig. 4. Relative energy level diagram for the dissociation of molecular hydrogen from protonated DHA calculated at the B3LYP/6-31G(d,p). (a) Both Hs are removed from C10 of $[DHA+H(1)]^+$. (b) Both Hs are removed from C10 of $[DHA+H(2)]^+$. In both (a) and (b) cationic 9-hydroanthracene is predicted as the final product.

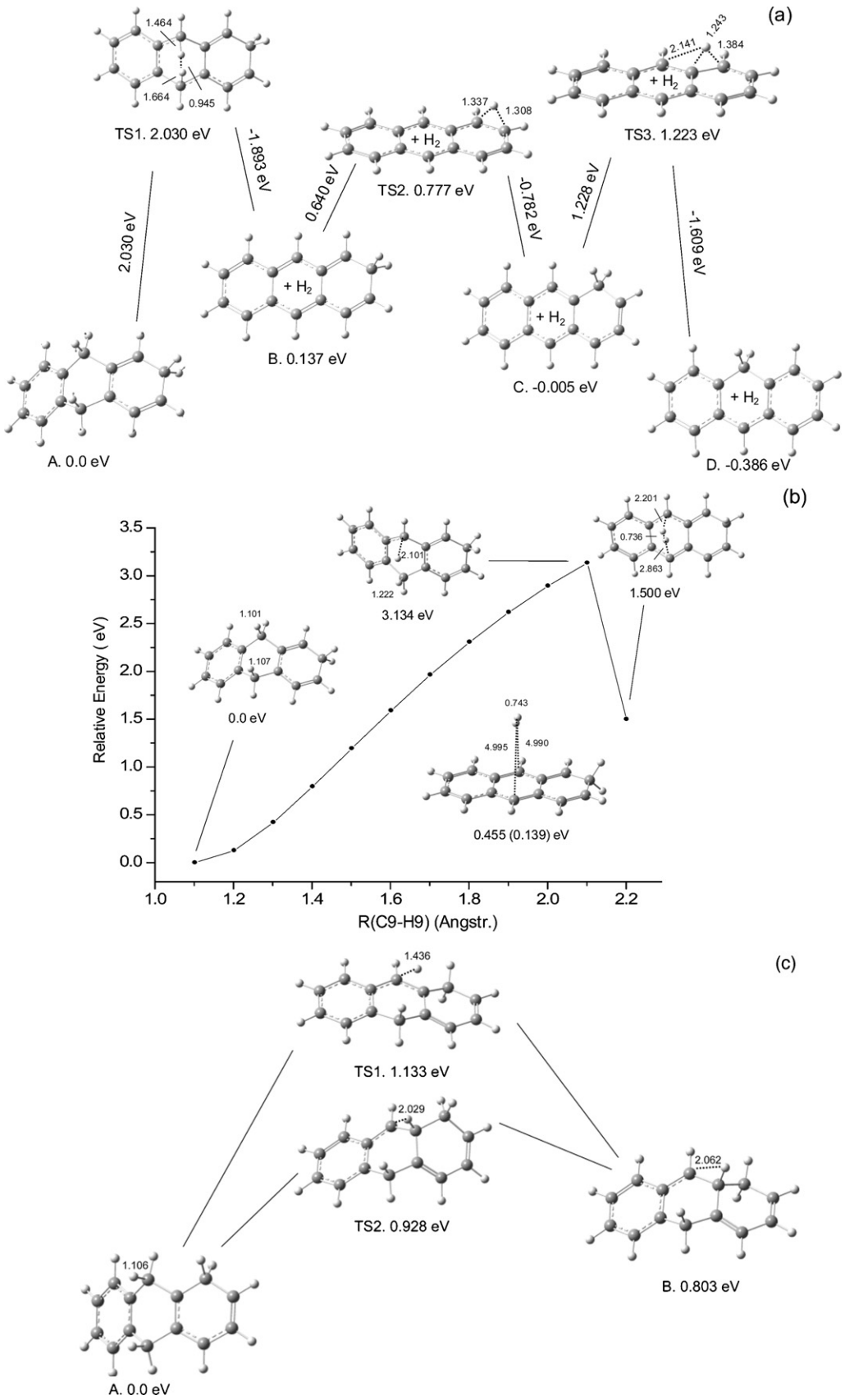

Fig. 5. Relative energy level diagram for the dissociation of molecular hydrogen from $[DHA+H(2)]^+$ calculated at the B3LYP/6-31G(d,p) level. (a) Both H9 and H10 hydrogens are supplied at the same time via vibration indicated by displacement vectors in reactant structure **A** (Hs rocking toward each other). (b) PES for C9–H9 bond lengthening. For each increment of the C9–H9 bond length, all other degrees of freedom were optimized. In this scan, the energy increases to 3.134 eV, with the lowest energy pathway directing H9 toward H10. Further incrementing the C9H9 bond leads to a drop in energy to 1.500 eV as the H–H bond starts to form. When this structure is fully optimized, the structure at the 0.455 eV relative energy is found. In contrast, when the C9–H9 bond length is incremented in $[DHA+H(1)]^+$, H9 is not directed to H10 but is trapped by the carbon bonded to C9 and C1 (c) forming the stable structure **B**.

the hydrogens in H_2 from C9 and C10 (~5 Å) and the H–H separation effectively signifies that molecular hydrogen has been formed and has dissociated from the aromatic parent. Note that although this structure was optimized, the vibrational frequency calculation finished with two imaginary frequencies indication an unstable structure. The 0.139 eV energy found is essentially the same as the energy found for structure **B** (in Fig. 5a), i.e., molecular H_2 and the 2-hydroanthracene cation.

Summarizing, H_2 may be formed from $[DHA+H(2)]^+$ by attraction of hydrogens originating from carbons across the middle six-membered ring (C9 and C10). Successive hydrogen atom shifts then occur and result in the final fragment product, the 9-hydroanthracene radical cation.

Although H_2 appears to form with relative ease from $[DHA+H(2)]^+$, the same cannot be said for $[DHA+H(1)]^+$. Fig. 5c gives the PES for the elongation of the C9H9 bond in $[DHA+H(1)]^+$. After mounting a relatively low barrier (1.1 eV) at **TS1**, the hydrogen hops to the inter-ring carbon between C9 and C1, and then, with a small increase in energy (~0.1 eV), hops back to C9. The whole structure then reverts to the more stable, original $[DHA+H(1)]^+$. In conclusion, H_2 may be formed via across-the-ring hydrogen pickup in $[DHA+H(2)]^+$, but not in $[DHA+H(1)]^+$.

3.4. PES calculations of hydrogen atom ejection from protonated DHA

To study the loss of a single H atom from protonated DHA, we incremented the C9H9 bond and found that the energy rises to 1.802 eV. After this it precipitously falls as the H atom jumps to an inter-ring carbon, which then adopts a distorted tetrahedral conformation (see Fig. 5c). From this position it hops back to C9. Ejection of a single H atom from protonated DHA is not feasible because, rather than escape the molecule, the H prefers to jump to an adjacent inter-ring carbon, finally reattaching to the C9 atom and reforming the original $[DHA+H(1)]^+$ reactant. This result is consistent with our finding that no fragment is obtained at m/z 180, i.e., loss of one mass unit.

3.5. IRMPD spectrum of the m/z 179 fragment

The m/z 179 fragment was predicted above to be the 9-hydroanthracene radical cation. If it could be established experimentally that this fragment was indeed the 9-hydroanthracene radical cation, it would support our theoretical approach.

The m/z 179 fragment was produced by collision-induced dissociation (CID) of the m/z 181 parent and isolating the fragment in the ICR cell. It should be recognized that the energy content of the m/z 179 fragment prepared by CID is different from one created by IRMPD. Our purpose in probing its structure is to corroborate (or not) the results of our calculations, all of which led to the 9-hydroanthracene ion as the photoproduct. The spectrum of the m/z 179 fragment, obtained by monitoring the intensity of the m/z 178 daughter ion as a function of infrared photon frequency from FELIX, is given in Fig. 6, where it is compared with the computed IR spectra of the three possible singly-protonated anthracenes: 9-hydroanthracene ($[An+H(9)]^+$), 1-hydroanthracene ($[An+H(1)]^+$), and 2-hydroanthracene ($[An+H(2)]^+$). Also given are their relative electronic ground state energies. The most stable isomer is $[An+H(9)]^+$, with $[An+H(1)]^+$ lying 0.378 eV higher and $[An+H(2)]^+$ at 0.511 eV. This order also reflects the site-specific proton affinities leading to these isomers: $[An+H(9)]^+$ (9.20 eV), $[An+H(1)]^+$ (8.83 eV), and $[An+H(2)]^+$ (8.69 eV) (B3LYP/6-31G++(d,p) level).

Of the three predicted IR spectra, it is clear that the spectrum of the $[An+H(9)]^+$ isomer most closely fits the observed one. The positions of all observed bands are well-reproduced by the predictions, although the relative intensities of the three bands in the 1400–1600 cm^{-1} region appear not to be well matched. This is however likely an experimental artifact caused by the slowly decreasing laser power toward higher frequencies. The IRMPD spectrum of protonated anthracene (m/z 179) has been previously reported by Dopfer and coworkers [21] and corresponds closely to the spectrum observed here. We conclude that the m/z 179 fragment produced in the infrared multiple photon irradiation of the parent protonated DHA is the 9-hydroanthracene cation. This finding is consistent with the present calculations which predict such a product after elimination of H_2 by any of several possible routes and corroborates our theoretical approach.

In addition to the m/z 179 fragment, other fragments at m/z 166 and 165 were also observed. The protonated parent (m/z 181) also loses 15 and 16 mass units in fragmentation. The former may be loss of CH_2 + H and the latter CH_2 + 2H. We suggest that the m/z 166 fragment results from the loss of CH_2 from the 9 or 10 position which then produces the fluorene radical cation [18] and the m/z 165 fragment is the dehydrogenated fluorene radical cation [22–24].

3.6. Relation to H_2 emission features in the ISM

In this and previous papers [11,12], we have determined that H_2 may be formed by excitation of hydrogenated PAHs. Previous work on protonated 1,2-dihydronaphthalene [11], acenaphthene, and 9,10-dihydrophenanthrene [12] showed that H_2 formation was possible in PAHs with adjacent aliphatic carbons and in this paper on 9,10-dihydroanthracene, we showed that adjacent groups are not necessary for H_2 formation.

In the calculations discussed above, the formation of molecular H_2 requires an energy input of 2–4 eV (see Figs. 3–5). At the **TS1** saddle point in each of these schemes, the soon-to-be-formed H_2 molecule undergoes an asymmetric extraction from its aliphatic carbon. For example, in Fig. 3a, the CH bond distances go from 1.104 and 1.092 Å to 1.615 and 2.296 Å at **TS1**, while the H–H length decreases from 1.753 Å to 0.790 Å at **TS1**. After a relaxation (−0.097 eV), a loose complex is formed with longer, but still unequal, CH distances (2.718 and 3.423 Å). The H–H separation has decreased to 0.746 Å in the complex. This situation is highly reminiscent of early work by Morokuma and coworkers on formaldehyde [25], who computed that the molecular photodissociation process leading to H_2 and CO goes through a highly asymmetric saddle point (different CH bond distances) and proposed that this indicated that the ejected H_2 was rotationally excited. Furthermore, they also pointed out that at the saddle point the H–H and CO separations were much closer to the H_2CO values than to the H_2 and CO values, thus forming an early transition state in the entrance channel of the reaction. Such early transition states typically lead to vibrationally excited products [26,27], as is thus expected for the ejected H_2 and CO from formaldehyde. Subsequent theoretical and experimental studies have borne out the prediction of rotational and vibrational excitation in both H_2 and CO [28,29], and new reports continue to appear [30]. Although formaldehyde and the PAH under study here are obviously very different in terms of degrees of freedom, etc., there is an intriguingly similar asymmetry of the transition state toward H_2 detachment.

As Figs. 3–5 indicate, the transition states through which protonated DHA passes are all asymmetric with respect to the CH lengths and show an H–H distance larger than found in H_2 (0.74 Å), suggestive of an early transition state. We therefore propose that as H_2 is ejected from protonated DHA it will be rotationally and vibrationally excited, and possibly also translationally excited. Since similar transition states were found in our previous calculations on H_2 ejection from protonated 1,2-dihydronaphthalene, acenaphthene, and 9,10-dihydrophenanthrene, we suggest that rotational

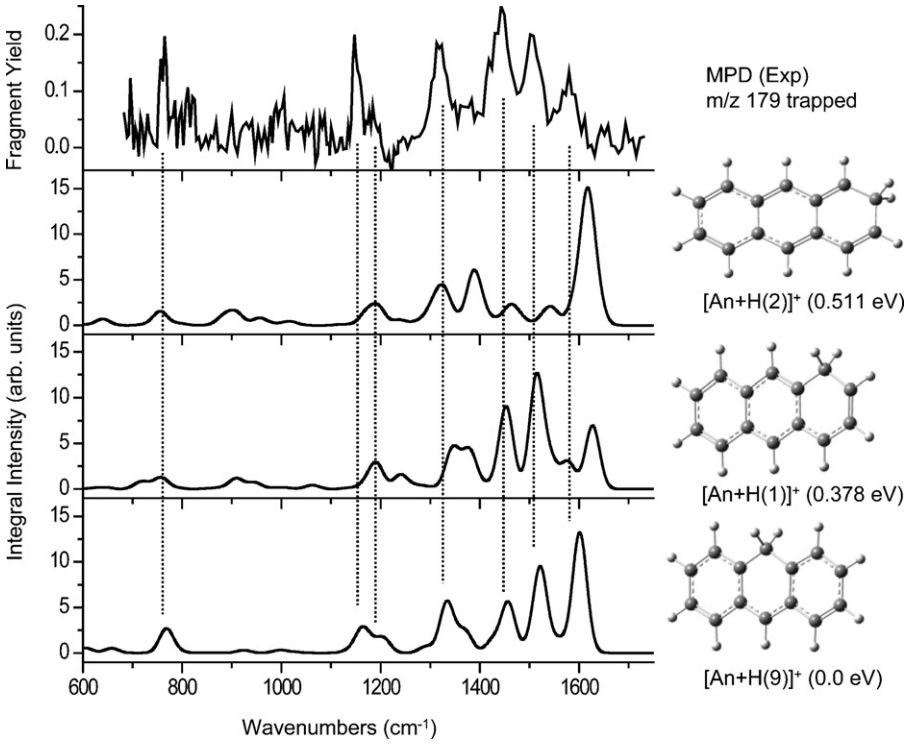

Fig. 6. Experimental IRMPD spectrum for the *m*/*z* 179 fragment obtained from the *m*/*z* 181 protonated DHA parent (top) compared to the predicted vibrational absorption spectra (at B3LYP/6-311++G(d,p) level) of the three isomers of protonated anthracene. The relative ZPE-corrected isomer electronic energies are indicated.

and vibrational excitation of H_2 is probably operative in them also. Further experimental and theoretical work will be necessary to determine the distribution of kinetic and rovibrational energies of the ejected H_2.

An important question remains: is there any evidence from astronomical observations that PAHs (or hydrogenated PAHs) are found in the same regions of interstellar space as H_2 and could the observed interstellar H_2 emission result from excitation via formation pumping?

A number of groups have presented evidence that hydrogenated PAHs may account for some of the spectral observations from the ISM. Recording infrared absorption spectra on Ar-matrix-isolated PAHs containing varying numbers of aliphatic hydrogens and comparing their spectra to various interstellar objects, Bernstein et al. [31] showed that in regions of high UV flux, such as the Orion bar, a good match in the 3.17–3.70 μm range is found for PAHs with a "modest" number of aliphatic hydrogens, whereas in regions of lower flux, such as IRAS 05341, a good match is found for methyl-PAHs or PAHs with high excess hydrogen coverage, i.e., superhydrogenated PAHs.

In their IR emission study of five gas-phase UV laser-excited hydrogenated PAHs, including acenaphthene and 9,10-dihydrophenanthrene (DHP), Saykally and coworkers [32] showed that the minor unidentified infrared (UIR) emission bands at 3.40, 3.46, and 3.51 μm from the Orion Bar [33] and IRAS 21282 + 5050 [34] are well-matched by the emission from DHP, although the intensity match of these bands to the major 3.3 μm band, usually ascribed to an aromatic CH stretch, was poor. They proposed that a larger species with more aromatic hydrogens, such as dihydrocircumcoronene ($C_{54}H_{20}$), which contains two adjacent aliphatic carbons, would better match the observed frequencies *and* intensities.

Recent studies have tracked the spatial coincidence of infrared PAH emission and H_2 emission in several interstellar objects. Using data from the Spitzer probe of the PDR around Monoceros R2, Berne et al. [35] investigated the spatial structure of emissions from ionized Ne, PAHs, and H_2 and found that, in this high UV field region, the H_2 lines did not precisely overlap with the PAH bands, but appeared more distant from the radiation source, as also found in the Orion bar PDR [36]. This is contrary to what is seen in low UV field PDRs like the Ophiucus filament [37] where they do overlap.

In their Spitzer Space telescope study of the aliphatic and aromatic components of PAH emission features from 53 Herbig Ae stars, Acke et al. [38] found that cool stars are surrounded by hydrocarbons with a high aliphatic/aromatic CH ratio and low CH/CC ratio, while the reverse was true for hot stars. They concluded that a strong UV flux decreases the aliphatic component of a hydrogenated PAH and enhances the aromatic component.

In spatial studies, Sloan et al. [39] found that the 3.41 μm UIR feature which matches the hydrogenated PAH spectra in the Orion bar region, coincides with the maximum in the H atom density. Furthermore, the H_2 emission is seen to lie precisely at the interface between the ionized HII and neutral HI regions. The authors state that this behavior is consistent with hydrogenated PAHs being produced by H atom addition in this region and surviving up to the PDR.

Several groups have observed broadening of the H_2 rotational lines with increasing J level which may result from excitation of H_2 via formation pumping. Jenkins and Peimbert [40] found that the rotational line widths increase with increasing J level toward the star ζ Ori A. Spitzer et al. [41,42], and LaCour et al. [43] reported similar findings while the latter authors showed that the high J rotational bands of H_2 toward four early-type Galactic stars exhibited velocity dispersion (band width *b*) increases with level of excitation. Since it was not possible to fit all J levels with a single *b* parameter, these authors proposed a mechanism where the broadening is due to the rotational excitation from excess energy acquired during H_2 formation on a grain. Although the model accounts for the different velocity dispersions, it requires a formation rate up to 10 times higher than the standard rate [44].

Summarizing, the model proposed here – the formation of H_2 from the photodissociation of hydrogenated PAHs – is consistent with a number of astronomical observations, but it is still incomplete. Hydrogenation of PAHs could occur in regions with sufficient H atom density such as near the Orion bar photodissociation region. Photoexcitation of the hydrogenated PAH would require a nearby stellar source. The rate at which H_2 could be formed will undoubtedly depend on the UV flux and energies. Given the energies in stellar sources, the energy that is in excess after crossing over the transition state for formation of the PAH–H_2 complex could appear as translational, rotational, and vibrational excitation of the ejected H_2. Further theoretical and experimental work is required to probe this mechanism in detail, i.e., to understand the internal conversion process and the branching of the excess energy into the various degrees of freedom of the ejected H_2, and to decide whether this approach is applicable to any of the observations made to date.

Acknowledgements

MV and JS gratefully acknowledge the support of the Petroleum Research Foundation, administered by the American Chemical Society, for its support of this research. JO acknowledges support from the NWO sponsored Dutch Astrochemistry Network and the Stichting Physica. The authors also thank the staff of the FOM Institute for Plasma Physics for its efficient operation of the FELIX free electron laser facility.

References

[1] R.J. Gould, E.E. Salpeter, The interstellar abundance of the hydrogen molecule. I. Basic processes, Astrophys. J. 138 (1963) 393–407.
[2] A. Omont, Physics and chemistry of interstellar polycyclic aromatic molecules, Astron. Astrophys. 164 (1986) 159–178.
[3] D.K. Bohme, PAH [polycyclic aromatic hydrocarbons] and fullerene ions and ion/molecule reactions in interstellar and circumstellar chemistry, Chem. Rev. 1487 (1992) 1487–1508.
[4] N.P. Cassam-Chenai, F. Pauzat, Y. Ellinger, Is stripping of polycyclic aromatic hydrocarbons a route to molecular hydrogen, AIP Conf. Proc. 312 (1994) 543–548.
[5] F. Pauzat, Y. Ellinger, The 3.2–3.5 μm region revisited – II. A theoretical study of the effects of hydrogenation on some model PAHs, Mon. Not. R. Astron. Soc. 324 (2001) 355–366.
[6] C.W. Bauschlicher, The reaction of polycyclic aromatic hydrocarbon cations with hydrogen atoms: the astrophysical implications, Astrophys. J. 509 (1998) L125–L127.
[7] M. Hirama, T. Tokosumi, T. Ishida, J. Aihara, Possible molecular hydrogen formation mediated by the inner and outer carbon atoms of typical PAH cations, Chem. Phys. 305 (2004) 307–316.
[8] E. Rauls, L. Hornekaer, Catalyzed routes to molecular hydrogen formation and hydrogen addition reactions on neutral polycyclic aromatic hydrocarbons under interstellar conditions, Astrophys. J. 679 (2008) 531–536.
[9] F. Jolibois, A. Klotz, F.X. Gadea, C. Joblin, Hydrogen dissociation of naphthalene cations: a theoretical study, Astron. Astrophys. 299 (2005) 629–634.
[10] V. Le Page, T.P. Snow, V.M. Bierbaum, Molecular hydrogen formation catalyzed by polycyclic aromatic hydrocarbons in the interstellar medium, Astrophys. J. 704 (2009) 274–280.
[11] M. Vala, J. Szczepanski, J. Oomens, J.D. Steill, H_2 ejection from polycyclic aromatic hydrocarbons: infrared multiphoton dissociation study of protonated 1,2-dihydronaphthalene, J. Am. Chem. Soc. 131 (2009) 5784–5791.
[12] J. Szczepanski, J. Oomens, J.D. Steill, M. Vala, H2 ejection from polycyclic aromatic hydrocarbons: infrared multiphoton dissociation study of protonated acenaphthene and 9,10-dihydrophenanthrene, Astrophys. J. 727 (12) (2011) 13.
[13] D. Oepts, A.F.G. van der Meer, P.W. van Amersfoort, The free-electron-laser user facility FELIX, Infrared Phys. Technol. 36 (1995) 297–308.
[14] J. Oomens, A.J.A. van Roij, G. Meijer, G. von Helden, Gas-phase infrared photodissociation spectroscopy of cationic polyaromatic hydrocarbons, Astrophys. J. 542 (2000) 404–410.
[15] J. Lemaire, P. Boissel, M. Henninger, G. Mauclaire, G. Bellec, H. Mestdagh, A. Simon, S. LeCaer, J.M. Ortega, F. Glotin, P. Maitre, Gas phase infrared spectroscopy of selectively prepared ions, Phys. Rev. Lett. 89 (2002) 273002.
[16] J.J. Valle, J. Eyler, J. Oomens, D.T. Moore, A.F.G. van der Meer, G. von Helden, G. Meijer, C.L. Hendrickson, A.G. Marshall, G.T. Blakney, Free electron laser-Fourier transform ion cyclotron resonance mass spectrometry facility for obtaining infrared multiphoton dissociation spectra of gaseous ions, Rev. Sci. Instrum. 76 (2005) 023103–023107.
[17] N.C. Polfer, J. Oomens, Reaction products in mass spectrometry elucidated with infrared spectroscopy, Phys. Chem. Chem. Phys. 9 (2007) 3804–3817.
[18] M.J. Frisch, G.W. Trucks, H.B. Schlegel, G.E. Scuseria, M.A. Robb, J.R. Cheeseman, J.A. Montgomery Jr., T. Vreven, K.N. Kudin, J.C. Burant, J.M. Millam, S.S. Iyengar, J. Tomasi, V. Barone, B. Mennucci, M. Cossi, G. Scalmani, N. Rega, G.A. Petersson, H. Nakatsuji, M. Hada, M. Ehara, K. Toyota, R. Fukuda, J. Hasegawa, M. Ishida, T. Nakajima, Y. Honda, O. Kitao, H. Nakai, M. Klene, X. Li, J.E. Knox, H.P. Hratchian, J.B. Cross, V. Bakken, C. Adamo, J. Jaramillo, R. Gomperts, R.E. Stratmann, O. Yazyev, A.J. Austin, R. Cammi, C. Pomelli, J.W. Ochterski, P.Y. Ayala, K. Morokuma, G.A. Voth, P. Salvador, J.J. Dannenberg, V.G. Zakrzewski, S. Dapprich, A.D. Daniels, M.C. Strain, O. Farkas, D.K. Malick, A.D. Rabuck, K. Raghavachari, J.B. Foresman, J.V. Ortiz, Q. Cui, A.G. Baboul, S. Clifford, J. Cioslowski, B.B. Stefanov, G. Liu, A. Liashenko, P. Piskorz, I. Komaromi, R.L. Martin, D.J. Fox, T. Keith, M.A. Al-Laham, C.Y. Peng, A. Nanayakkara, M. Challacombe, P.M.W. Gill, B. Johnson, W. Chen, M.W. Wong, C. Gonzalez, J.A. Pople, Gaussian, Inc., Gaussian 03, Rev. B. 05, Gaussian, Inc., Wallingford CT, 2004.
[19] M. Vala, J. Szczepanski, R. Dunbar, J. Oomens, J.D. Steill, Infrared multiphoton dissociation spectrum of isolated protonated 1-azapyrene, Chem. Phys. Lett. 47 (2009) 43–48.
[20] J. Oomens, B.G. Sartakov, G. Meijer, G. Von Helden, Gas-phase infrared multiple photon dissociation spectroscopy of mass-selected molecular ions, Int. J. Mass Spectrom. 254 (2006) 1–19.
[21] H. Knorke, J. Langer, J. Oomens, O. Dopfer, Infrared spectra of isolated protonated polycyclic aromatic hydrocarbon molecules, Astrophys. J. 706 (2009) L66–L70.
[22] J. Szczepanski, J. Banisaukas, M. Vala, S. Hirata, R.J. Bartlett, M. Head-Gordon, Vibrational and electronic spectroscopy of the fluorene cation, J. Phys. Chem. A 106 (2002) 63–73.
[23] J. Szczepanski, J. Banisaukas, M. Vala, S. Hirata, W.R. Wiley, Preresonance Raman spectrum of the $C_{13}H_9$ fluorene-like radical, J. Phys. Chem. A 106 (2002) 6935–6940.
[24] J. Oomens, G. Meijer, G. van Helden, Gas-phase infrared spectroscopy of cationic indane, acenaphthene, fluorene, and fluoranthene, J. Phys. Chem. A 105 (2001) 8302–8309.
[25] R.L. Jaffe, D.M. Hayes, K. Morokuma, Photodissociation of formaldehyde: potential energy surfaces for $H_2CO \rightarrow H_2 + CO$, J. Chem. Phys. 60 (1974) 5108–5109.
[26] J.C. Polanyi, Some concepts in reaction dynamics, Acc. Chem. Res. 5 (1972) 161–168.
[27] R.D. Levine, R.B. Bernstein, Molecular Reaction Dynamics and Chemical Reactivity, Oxford University Press, New York, 1987, pp. 117–206.
[28] T.J. Butenhoff, K.L. Carleton, C.B. Moore, Photodissociation dynamics of formaldehyde: H_2 rotational distributions and product state correlations, J. Chem. Phys. 92 (1990) 377–393.
[29] R.D. van Zee, M.F. Foltz, C.B. Moore, Evidence for the second molecular channel in the fragmentation of formaldehyde, J. Chem. Phys. 99 (1993) 1664–1673.
[30] B.C. Shepler, E. Epifanovsky, P. Zhang, J.M. Bowman, A.I. Krylov, K. Morokuma, Photodissociation dynamics of formaldehyde initiated at the T_1/S_0 minimum energy crossing configuration, J. Phys. Chem. A 112 (2008) 13267–13270.
[31] M.P. Bernstein, S.A. Sanford, L.J. Allamandola, Hydrogenated polycyclic aromatic hydrocarbons and the 2940 and 2850 wavenumber (3.40 and 3.51 micron) infrared emission features, Astrophys. J. 472 (1996) L127–L130.
[32] D.R. Wagner, H.S. Kim, R.J. Saykally, Peripherally hydrogenated neutral polycyclic aromatic hydrocarbons as carriers of the 3 micron interstellar infrared emission complex: results from single-photon infrared emission spectroscopy, Astrophys. J. 545 (2000) 854–860.
[33] T.R. Geballe, A.G.G.M. Tielens, L.J. Allamandola, A. Moorhouse, P.W.J.L. Brand, Spatial variations of the 3 micron emission features within the UV-excited nebulae: photochemical evolution of interstellar polycyclic aromatic hydrocarbons, Astrophys. J. 341 (1989) 278–287.
[34] M. deMuizon, T.R. Geballe, L.B. d'Hendecourt, F. Baas, New emission features in the infrared spectra of two IRAS sources, Astrophys. J. 306 (1986) L105–L108.
[35] O. Berne, A. Fuente, J.R. Goicoechea, P. Pilleri, M. Gonzalez-Garcia, C. Joblin, Mid-infrared polycyclic aromatic hydrocarbon and H_2 emission as a probe of physical conditions in extreme photodissociation regions, Astrophys. J. 706 (2009) L160–L163.
[36] A.G.G.M. Tielens, M.M. Meixner, P. van der Werf, J. Bregman, J.A. Tauber, J. Stutzki, D. Rank, Anatomy of the photodissociation region in the Orion Bar, Science 262 (1993) 86–89.
[37] E. Habart, A. Abergell, C.M. Walmsley, D. Teyssier, J. Pety, Density structure of the Horsehead nebula photodissociation region, Astron. Astrophys. 437 (2005) 177–188.
[38] B. Acke, J. Bouwman, A. Juhasz, Th. Henning, M.E. van der Ancher, G. Meeus, A.G.G.M. Tielens, L.B.F.M. Waters, Spitzer's view on aromatic and aliphatic hydrocarbon emission in Haerbig Ae stars, Astrophys. J. 718 (2010) 558–574.
[39] G.C. Sloan, J.D. Bregman, T.R. Geballe, L.J. Allamandola, C.E. Woodward, Variations in the 3 micron spectrum across the Orion Bar: polycyclic aromatic hydrocarbons and related molecules, Astrophys. J. 474 (1997) 735–740.
[40] E.B. Jenkins, A. Peimbert, Molecular hydrogen in the direction of ζ Orionis A, Astrophys. J. 477 (1997) 265–280.
[41] L. Spitzer, W.D. Cochran, Rotational excitation of interstellar H_2, Astrophys. J. 186 (1973) L23–L28.
[42] L. Spitzer, W.D. Cochran, A. Hirshfeld, Column densities of interstellar molecular hydrogen, Astrophys. J. Suppl. 28 (1974) 373–389.
[43] S. LaCour, V. Ziskin, G. Hebrard, C. Oliveira, M.K. Andre, R. Ferlet, A. Vidal-Madjar, Velocity dispersion of high rotational levels of H_2, Astrophys. J. 627 (2005) 251–262.
[44] M. Jura, Interstellar clouds containing optically thin H_2, Astrophys. J. 197 (1975) 575–580.